Earth Planet. Sci. Lett. 643 (2024) 118906



Contents lists available at ScienceDirect

Earth and Planetary Science Letters

journal homepage: www.elsevier.com/locate/epsl





Tracking quartz and zircon provenance in sedimentary rocks using Ti distributions: Unlocking the volcanic-plutonic connection in old igneous systems

L.M. Fonseca Teixeira [a,b,*], O. Laurent [c], J. Troch [b], C.S. Siddoway [d], L. Tavazzani [a], C. Deering [e], O. Bachmann [a]

[a] Department of Earth Sciences, ETH Zürich, 8092, Zurich, Switzerland
[b] Division of Earth Sciences and Geography, RWTH Aachen University, 52072, Aachen, Germany
[c] CNRS, Observatoire Midi-Pyrénées, Géosciences Environnement Toulouse, 31400, Toulouse, France
[d] Department of Geology, Colorado College, Colorado Springs, CO, 80903, USA
[e] Department of Geological and Mining Engineering and Sciences, Michigan Technological University, Houghton, MI, 49931, USA

ARTICLE INFO

Editor: Dr C. M. Petrone

Keywords:
Volcanic-plutonic connection
Ti-in-quartz
Ti-in-zircon
Pikes Peak batholith
Sedimentary provenance

ABSTRACT

Although the relationship between silicic volcanic and plutonic rocks has been extensively studied, it remains controversial whether most plutons have volcanic counterparts and how the volcanic-to-plutonic ratio has evolved through time. This stems primarily from the scarcity of geologic examples with both volcanic and plutonic counterparts, especially in ancient terranes where volcanic deposits have likely been eroded. Here, we introduce a novel approach to identify remnant volcanic crystals in proximal siliciclastic/detrital rock formations. As most erupted crystals stop their growth before reaching the solidus, in contrast to plutonic crystals, the distribution of Ti (a proxy for temperature of crystallisation and/or magma evolution) in (weathering-resistant) quartz and zircon can help in identifying volcanic crystals in sedimentary rocks derived from supracrustal sources that have been completely eroded. Laser-ablation inductively coupled plasma-mass spectrometry (LA-ICP-MS) analyses of quartz and zircon from volcanic and plutonic units that are known to be spatially and temporally related (from Southern Rocky Mountain Volcanic Field, Colorado, and Taupo Volcanic Zone, New Zealand) reveal that volcanic crystals have generally distinct distributions of, and on average higher Ti contents than, plutonic crystals. To further develop and test this methodology, we analysed samples from the 1.075 Ga Pikes Peak granite (CO, USA) and from the associated series of intra-granite sedimentary dikes that form part of the Cryogenian Period Tava sandstone. Blue band cathodoluminescence (CL) images can be used as a proxy for Ti-in-quartz. Our CL-screening method provides a statistically representative distribution of Ti contents in quartz crystals from individual thin sections. The Tava sandstone contains a higher concentration of high-Ti (and hence high-temperature) quartz and zircon grains than the average Pikes Peak batholith, interpreted as grains eroded from a no longer exposed, volcanic counterpart of the Pikes Peak magmatic system. Our study illustrates a means to test whether magmatic reservoirs that are now represented by crystallised ancient plutons once fed volcanic eruptions, and identifies a strategy for reconstructing volcanic-plutonic relationships, even when parts of the geological association have been eroded.

1. Introduction

For centuries, the relationship between silicic volcanic and plutonic rocks has been debated, starting with the work of James Hutton in the late 1700s. Although the volcanic-plutonic connection is considered an axiom for mafic rocks, with mafic plutons widely accepted as cumulates in many instances (since the work of Wager et al., 1960), up to now, the existence of silicic cumulates and the importance of plutonic-volcanic connections remain controversial. Recent studies addressed the numerous arguments for or against the volcanic-plutonic connection in silicic rocks (Bachmann et al., 2007; Bachmann and Huber, 2016; Glazner et al., 2018; Clemens et al., 2022; Wallrich et al., 2023).

* Corresponding author.
E-mail address: ludmila.fonseca@erdw.ethz.ch (L.M. Fonseca Teixeira).

https://doi.org/10.1016/j.epsl.2024.118906
Received 6 May 2024; Received in revised form 15 July 2024; Accepted 20 July 2024
Available online 7 August 2024
0012-821X/© 2024 The Authors. Published by Elsevier B.V. This is an open access article under the CC BY license (http://creativecommons.org/licenses/by/4.0/).

Supporting a co-genetic link, "kinships" that connect plutonic and volcanic realms (Bachmann et al., 2007) include:

1. Spatial and temporal kinship: in magmatic provinces where plutons are exposed by erosion, volcanic and plutonic rocks of the same age have been found (e.g. Sesia Magmatic System, Italy, Quick et al., 2009; Karakas et al., 2019; Takidani pluton in Japan, Hartung et al., 2021; Farina et al., 2024; the Campo Alegre-Corupá Basin in Brazil, Martins Lino et al., 2023; Early Andean Magmatic Province in Chile, Oliveros et al., 2006; White Mountain magma series, Kennedy and Stix, 2007; Southern Rocky Mountain volcanic field, Lipman, 2007; Turkey Creek in Arizona, Deering et al., 2016, Searchlight-Highland Range system, Wallrich et al., 2023) .
2. Geochemical and petrological kinships: volcanic and plutonic rocks that are spatially and temporally related have similar and/or complementary whole-rock compositions, as well as similar mineral assemblages and ranges in isotopic ratios (e.g.Barth et al., 1993; Metcalf et al., 1995; Deering et al., 2016).
3. Geophysical kinship: large silicic crystal-rich magma reservoirs have been identified beneath various active calderas through negative gravity anomalies (e.g. Heiken et al., 1990; De Silva et al., 2006), magnetotelluric (Heise et al., 2010), and seismic experiments (e.g. Wilson et al., 2003; Ward et al., 2014; Delph et al., 2017).

Owing to the architecture of magmatic systems, exposed examples with both volcanic and plutonic counterparts are rare, so the previously mentioned arguments are mainly derived from the study of relatively young (i.e. Mesozoic and younger) systems. Exceptions are tilted crustal sections (e.g. the Permian Sesia Magmatic System in NW Italy; Quick et al., 2009; Tavazzani et al., 2020, 2023) or unroofed plutonic domains with preserved associated volcanic rocks (e.g. the Paleoarchean Barberton TTGs and silicic volcanics; Laurent et al., 2020, 2022). The prevalence of plutons in pre-Mesozoic crust begs the question of whether (1) older systems underwent more erosion, alteration and/or overprinting metamorphic processes, leading to systematic removal of volcanic formations, or (2) older pluton formation was not systematically associated with volcanism, and instead suggests a lower volcanic: plutonic ratio for the Early Earth. The volcanic:plutonic ratio is also an important parameter for evaluating the mechanisms of Earth's internal heat dissipation, i.e. global geodynamic systems (Crisp, 1984; Rozel et al., 2017). Therefore, the inherent limitations and preservation bias in the crustal record prevent the understanding of the volcanic-plutonic connection throughout Earth's history and leave key questions unanswered: Do all plutons have a volcanic counterpart? If not, what proportion of them were associated with an eruptive stage? Has the volcanic:plutonic ratio changed during Earth's history and if so, what does it imply about the geodynamic evolution of the planet?

When volcanic strata are eroded, the resulting detrital sediments may preserve parts of the extrusive record. In ancient lithologies, however, many of the original crystals may have been affected by post-crystallisation alteration. Likely to survive are quartz and zircon, both common in evolved, silicic volcanic rocks and resistant to chemical and mechanical weathering. Therefore, they are likely the best candidates to preserve information on the original magmatic conditions (e.g. Stalder et al., 2017) and to occur as volcanic remnants in the sedimentary record. Their trace element concentrations can be used for geothermometry, notably Ti-in-quartz (e.g. Wark and Watson, 2006; Huang and Audétat, 2012; Osborne et al., 2022), and Ti-in-zircon (Ferry and Watson, 2007; Loucks et al., 2020; Crisp et al., 2023), and thus help to constrain crystallisation temperatures, a parameter that can be used to statistically distinguish volcanic, plutonic, and pegmatitic/hydrothermal crystals (see next section). Therefore, determining the distribution of Ti contents in representative quartz and zircon populations in siliciclastic rocks represents a promising tool to investigate the plutonic-volcanic connection throughout Earth's history.

In this study, we establish the differences in Ti distribution between plutonic and volcanic quartz and zircon through forward modelling and direct analysis of two well-studied modern silicic magmatic systems (Colorado Southern Tocks Mountain Volcanic Field, USA; and the Taupo Volcanic Zone, New Zealand). Having established these differences, we use the Pikes Peak batholith (1.075 Ga; Smith, 1999) and spatially related sediments of the Tava Sandstone to develop a method to identify contributions from ancient, no longer present volcanic units. The Tava sandstone formed ca. 676 Ma (Jensen et al., 2018) and incorporated detritus eroded from Proterozoic basement, including a large population of 980–1100 Ma zircon (Siddoway and Gehrels, 2014).

We employ a novel approach based on Ti-thermometry to statistically assess the provenance of detrital quartz and zircon, and thus allow fingerprinting of coeval volcanic, plutonic, and hydrothermal/pegmatitic contributions to the sedimentary record. We measure the Ti contents of quartz using LA-ICP-MS, and calibrate the Ti values to the blue band cathodoluminescence (CL) properties of quartz, to enable classification of large quartz populations in thin section. Numerous studies have observed that quartz CL intensity directly correlates with Ti concentrations (e.g. Rusk et al., 2006; Spear and Wark, 2009). Although other elements (e.g. Al) can influence CL in quartz, their impact is generally less significant (Müller et al., 2003). As a result, Ti contents of a representative population of quartz crystals (i.e. hundreds or thousands of grains in an individual thin section) can be analysed in a relatively fast, convenient, and cost-efficient manner. Our study of post magmatic sedimentary rocks identifies detrital grains (zircon, quartz) having the Ti content that is diagnostic of erupted units, as distinct from grains derived from plutonic and hydrothermal/pegmatitic sources. The technique shows promise for identification of the 'missing' supracrustal component of ancient igneous systems, and a means to advance our understanding of volcanic-plutonic processes.

1.1. Rationale of the Ti-based method to investigate the volcanic-plutonic connection

A key distinction between silicic volcanic and plutonic rocks is their thermal history. Volcanic eruptions typically sample the mobile, high temperature, melt-rich part of magma reservoirs, which therefore usually registers temperatures higher than the solidus. Some crystals in volcanic units can be recycled from lower-temperature wall rocks (xenocrysts) or crystalline rinds on the edge of the magma chambers (Miller et al., 2007; Ellis et al., 2014; Siégel et al., 2018; Troch et al., 2018; Szymanowski et al., 2019), but they should not be dominant in terms of volume. In contrast, plutons crystallise to completion and ordinarily are comprised of minerals that record extended cooling until the solidus. In some instances, late saturated magmatic volatile phase and/or residual melts rich in fluxing elements may generate peri-plutonic systems (hydrothermal veins, pegmatites) recording temperatures even below those of the typical wet granite solidus (e.g. Fonseca Teixeira et al., 2022). Subsolidus recrystallisation of igneous plutonic minerals would record similar temperature ranges. Of course, plutons may preserve some high-temperature minerals, and volcanic rocks may contain ante- and/or xenocrysts recording low temperatures, but statistically, temperature estimates of plutonic rocks can be expected to be skewed towards lower temperatures compared to volcanic units for a given mineral phase and comparable bulk rock compositions.

Two minerals that have high preservation potential and crystallise commonly in high-silica magmas are quartz and zircon. Ti contents in both minerals record crystallisation temperatures (see references above). In simple terms, for a given $a\mathrm{TiO_2}$ ($a\mathrm{TiO_2}^{\text{liquid-rutile}}$, or the $a\mathrm{TiO_2}$ in the melt relative to rutile saturation), quartz/zircon formed at higher temperatures have higher Ti contents than crystals formed at lower temperatures (e.g. Wark and Watson, 2006; see Introduction for other references). During volcanic activity, eruption of quartz and/or zircon-saturated magma leads to extraction of these phases from a magma body before it has fully solidified. For the plutonic residual, two possible crystallisation scenarios arise: (1) crystals nucleate prior to and

continue crystallising beyond an eruption, forming minerals with pre-eruptive cores overgrown by a post-eruptive rim, and (2) crystals that only begin to grow after material loss to an eruption. Consequently, a partial overlap in the crystallisation temperatures and in the Ti content of plutonic and volcanic quartz and zircon should occur, but their statistical distribution is expected to differ. Both minerals initiate crystallisation when the melt becomes saturated with the respective component, but volcanic crystals stop growing upon eruption, preventing their Ti content from reaching the lower near-solidus values found in plutonic crystals. Therefore, we hypothesize that the distribution of Ti in detrital quartz and zircon from siliciclastic sedimentary rocks should on the first order reflect the relative proportions of volcanic, plutonic, and hydrothermal/pegmatitic sources that fed the sedimentary system.

2. Geological background

2.1. The Pikes Peak batholith and associated rocks

The 1.075 Ga Pikes Peak batholith is an A-type granitic intrusion in the southern Colorado Front Range (Barker et al., 1975; Wobus et al., 1976; Smith, 1999). It covers an area of 3100 km^2 with the longer axis reaching 100 km, but more than half of the batholith might be unexposed (Tweto et al., 1980). It comprises alkali feldspar granite with biotite, hornblende, magnetite, ilmenite, and occasionally, allanite and fluorite. Zircon and apatite are common accessory phases. Pegmatites are abundant, many of which are enriched in REE. Although no volcanic rocks *sensu strictu* have been reported around the Pikes Peak batholith, the presence of the Keeton Porphyry, a small subvolcanic rhyodacitic body spatially and temporally associated with the Pikes Peak batholith (Sanders, 1999), suggests magmatic activity was not limited to pluton formation.

The batholith hosts the Tava sandstone "injectites" (Fig. 1), a series of Cryogenian intra-granite sedimentary dikes of up to 6 m in width that consist primarily of quartz (95 %) with subsidiary feldspar, mica, magnetite, and zircon (Siddoway and Gehrels, 2014). The Tava sandstone "injectites" (clastic dikes) formed approximately at 676 ± 26 Ma (Jensen et al., 2018), under conditions of catastrophic fluid overpressure that caused liquefaction and injection of sediments that were derived largely from Proterozoic igneous sources (Siddoway et al., 2013). The most likely cause of such over-pressure events is ground acceleration induced by earthquakes (Jonk, 2010), possibly triggered along the ancestral Ute Pass Fault (Siddoway, 2023). Detrital zircon ages (Siddoway and Gehrels;2014; Jensen et al. 2018) show significant populations of zircon grains between 980 and 1100 Ma.

2.2. Colorado southern rocky mountain volcanic field (SRMVF)

The SRMVF is an area within in Colorado and northern New Mexico known for hosting many voluminous ignimbrites and associated plutonics rocks, all yielding ages between 37 Ma and 26 Ma, with an estimated volume greater than 50,000 km^3 (Lipman, 2007). In this study, we focus on the following volcanic-plutonic systems, considered to be connected due to their spatial and geochronological kinship:

- Wall Mountain Tuff-Mount Princeton batholith (~37 Ma): The Wall Mountain Tuff, a crystal-rich rhyolite, erupted from vents above the granodioritic Mount Princeton batholith (Lipman, 2007; Zimmerer and McIntosh, 2012).
- Lake City Caldera (~23 Ma): this complex encompasses resurgent quartz syenite and the Sunshine Peak Tuff (SPT). The lower and middle SPT units are crystal-poor rhyolites, and the upper SPT is a crystal-rich trachyte (Lubbers et al., 2020; Pamukçu et al., 2022).
- San Luis Caldera (~27 Ma): Several volcanic units are associated with this caldera, including the dacitic Nelson Mountain tuff, the rhyolitic Rat Creek tuff, and the Captive Inca dacite (Lipman and Sawyer, 1988). Their plutonic counterpart is a resurgent granodiorite (Lipman, 2007).
- Bonanza Caldera (~33 Ma): the andesitic-to-rhyolitic Bonanza tuff is associated with the granodioritic Turquoise Mine pluton (Lipman et al., 2015).

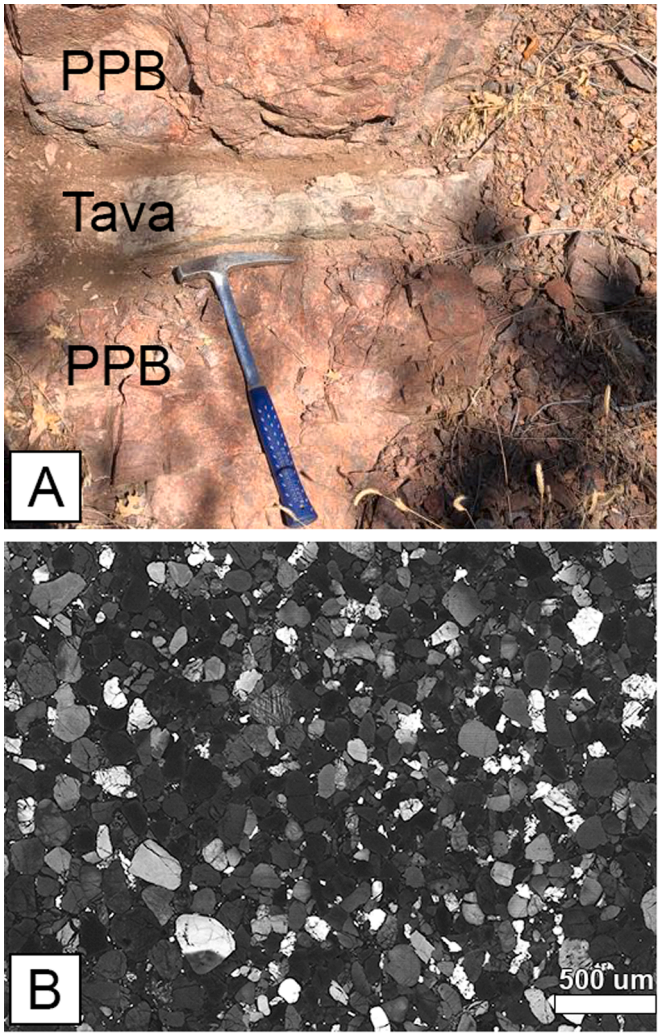

Fig. 1. (A) Tava sandstone dike hosted by Pikes Peak Granite(PPB). (B) Example CL image of a Tava Sandstone thin section (110–5A). The image shows mostly (95%) quartz crystals with variable brightness.

2.3. Taupo volcanic zone (TVZ)

The 300 km long TVZ in New Zealand includes one of the most active rhyolitic volcanic complexes on Earth (Wilson et al., 2009). The TVZ is comprised of multiple caldera complexes. Many of the ignimbrites and tephra deposits include comagmatic plutonic lithics (Brown et al., 1998) that allow for direct comparison of cogenetic volcanic and plutonic lithologies (Brown et al., 1998). For this study, we focused on the following locations (Brown et al., 1998; Graeter et al., 2015):

- Okataina volcanic complex containing granitoid lithics from the Karahoa and Rotoiti ignimbrites.
- Ohakuri caldera with granitoid lithics from the Ohakuri ignimbrite.

3. Methods

3.1. Linking cathodoluminescence images to Ti-in-quartz

In order to obtain statistically representative Ti-in-quartz distributions for sedimentary samples, we developed a method of calibration of Ti contents against cathodoluminescence (CL) response (see Leeman et al., 2012 for calibration at the scale of a single quartz grain). This allows one to obtain the Ti content distribution across an entire thin section within ca. 6 h, whereas the same time would allow a maximum of a few hundred point analyses (e.g. via LA-ICP-MS), at a significantly higher running cost.

Full thin section CL images of the Tava Sandstone were acquired at the Géosciences Environnement Toulouse laboratory of the Observatoire Midi-Pyrénées (GET-OMP) in Toulouse, France with a Tescan Vega4 Scanning Electron Microscope (SEM) equipped with a Tescan Rainbow-CL detector, acquiring red, blue, green, and panchromatic images simultaneously. Brightness and contrast were calibrated based on blue band emissions (300–500 nm), as this wavelength range is most sensitive to Ti content of quartz (Spear and Wark, 2009). Feldspars and other accessory phases were identified with EPMA BSE and aluminium WDS maps acquired with a JEOL JXA iSP 100 superprobe at RWTH Aachen University, using a pixel size of 10 μm, at 15 kV acceleration voltage. The step-by-step treatment to remove feldspars and the sedimentary matrix is described in the U Material.

For the calibration of Ti contents against CL response, 68 individual quartz crystals were measured in the thin section, via femtosecond laser-ablation inductively coupled plasma-mass spectrometry (fs-LA-ICP-MS) at GET-OMP (see Supplementary Material for further details). Quartz crystals were chosen to represent the span from very low to very high brightness in the CL intensity range. After excluding faulty points (e.g. feldspars, cracked crystals, uneven signals), 49 crystals were included in the calibration. The calibration curve was constructed by fitting the Ti contents obtained from fs-LA-ICP-MS with CL brightness values on the same spots obtained from CL images using the ®MATLAB Curve Fitting toolbox. The robustness of the CL-based calibration was assessed by an independent comparison of the results with statistical distributions of Ti contents analysed by fs-LA-ICP-MS in two smaller areas of the same thin section (~300 grains in each area).. In each area, the points correspond to a specific pattern:

(1) **Grid pattern** (n = 332), in which points were automatically distributed over a regular (200 μm-spaced) grid, which accepts more than one point inside a crystal.
(2) **Single grain pattern** (n = 286), in which one point was measured per grain, on randomly chosen grains, disregarding size.

3.2. Analysis of Ti contents in zircon and quartz

Zircons from the Pikes Peak batholith, the Keeton Porphyry and the Tava sandstone were separated using traditional mineral separation procedures (crushing, sieving, heavy liquids separation, magnetic separation, and picking under a binocular microscope). Zircons were annealed for ~ 60 h at 900 °C in a muffle furnace. Zircon mounts from volcanic-plutonic pairs from the SRMVF were provided by J. Sliwinski. Data from the original dataset (Sliwinski et al., 2022) is also utilised in this study (see Supp. for detailed information). SEM-CL images were acquired at ETHZ to help avoiding potential inherited cores. Following image acquisition, we analysed 50 to 200 points for each sample, including rim and core of mounted grains. Zircon U-Pb ages and trace element measurements were acquired simultaneously via LA-ICP-MS at ETHZ. We note that our Ti data uncertainty is ~5 % relative.

Zircons in the sandstone were filtered by: (1) considering only zircons with ages similar to the Pikes Peak batholith (1000–1150 Ma), and (2) selecting only zircons with euhedral shapes, to exclude zircon from distal sources that could yield similar ages to the Pikes Peak system (e.g. Siddoway and Gehrels, 2014). By filtering, we selected for zircon likely to originate in the Pikes Peak system when identifying high Ti grains.

Additionally, we analysed quartz from the Keeton Porphyry, and the TVZ and coeval plutonic lithics as a baseline for expected CL behaviour on volcanic versus plutonic quartz. Further information on all zircon and quartz analyses is available in the Supplementary Material.

3.3. Modelling of zircon Ti distributions in volcanic-plutonic pairs

To better illustrate the distribution between volcanic and plutonic crystals, and to help interpret the observed in natural data, we simulated hypothetical zircon Ti distributions for different zircon and quartz crystallisation histories and eruption temperatures. We calculated Ti contents for quartz and zircon crystallising within a magma body as temperature decreases. For volcanic minerals, crystallisation stops upon eruption and thus removal of a given fraction of mobile zircon/quartz-bearing magma. Plutonic crystals comprise non-erupted zircon leftover after eruption, as well as crystals growing upon further cooling of the reservoir. Our model counts number of crystals formed between 850 and 680 °C, at $a\mathrm{SiO_2} = 1$, and a pressure of 400 MPa (crystallisation pressure estimated for a significant part of the Pikes Peak batholith; Fonseca Teixeira et al., 2022). Ti contents in zircon are based on the calibration of Loucks et al. (2020). In quartz, Ti is estimated using the calibration of Huang and Audétat (2012). The model can trigger eruption based on a given temperature or percentage of crystallised minerals. The following variables were tested for their effect on the Ti distribution curves:

1. Number of crystals formed per 1 °C: Two cases were tested: 1) linear (1000 crystals per 1 °C), and 2) an exponential curve (see Supplementary Data for further information).
2. Fraction of erupted crystals (percentage of erupted crystals from total in magma chamber). The following eruption fractions were tested: 1 %, 5 %, 10 %.
3. $a\mathrm{TiO_2}$: 0.3, 0.5, 1.0.
4. Percentage of crystallised minerals (and consequently, eruption temperature): the percentage of zircon or quartz formed in the magma chamber at the time of eruption (100 % corresponds to no eruption): 40 %, 50 %, 60 %, 70 %, 80 %.

Additionally, we attempted to match our models with the natural data obtain from quartz (TVZ) and zircon (SRMVF) from natural systems. For these simulations, we chose an exponential crystallisation rate, as it matches better the shape of the observed natural zircon distribution. In order to reproduce the natural data, we further adjusted the pressure, $a\mathrm{TiO_2}$, $a\mathrm{SiO_2}$, solidus, saturation, and eruption temperature.

4. Results

4.1. Natural and modelled Ti distributions in zircon and quartz from modern volcanic-plutonic systems

For zircon, all case studies but Lake City Caldera show at least a small statistical gap between populations in which the volcanic crystals have a higher Ti content than their plutonic counterparts. The gap (Fig. 2) becomes more apparent in pairs with higher Ti contents (Mount Princeton). In lower Ti examples, the gap is narrow and can be better appreciated from density plots (Fig. 2): in Bonanza Caldera, volcanic crystals peak at 15 ppm Ti, and plutonic at 10 ppm; in San Luis Caldera, volcanic crystals peak at 6 ppm, and plutonic at 3 ppm.

A similar pattern is seen in Ti distribution in quartz crystals: data from quartz in volcanic units and in lithic plutonic clasts from TVZ also show that volcanic and plutonic quartz are statistically distinct, in that the distribution of volcanic crystals is enriched in Ti (peaking at ~75 ppm) relative to those from co-erupted plutonic crystals (peaking at ~ 60 ppm Ti; Fig. 3).

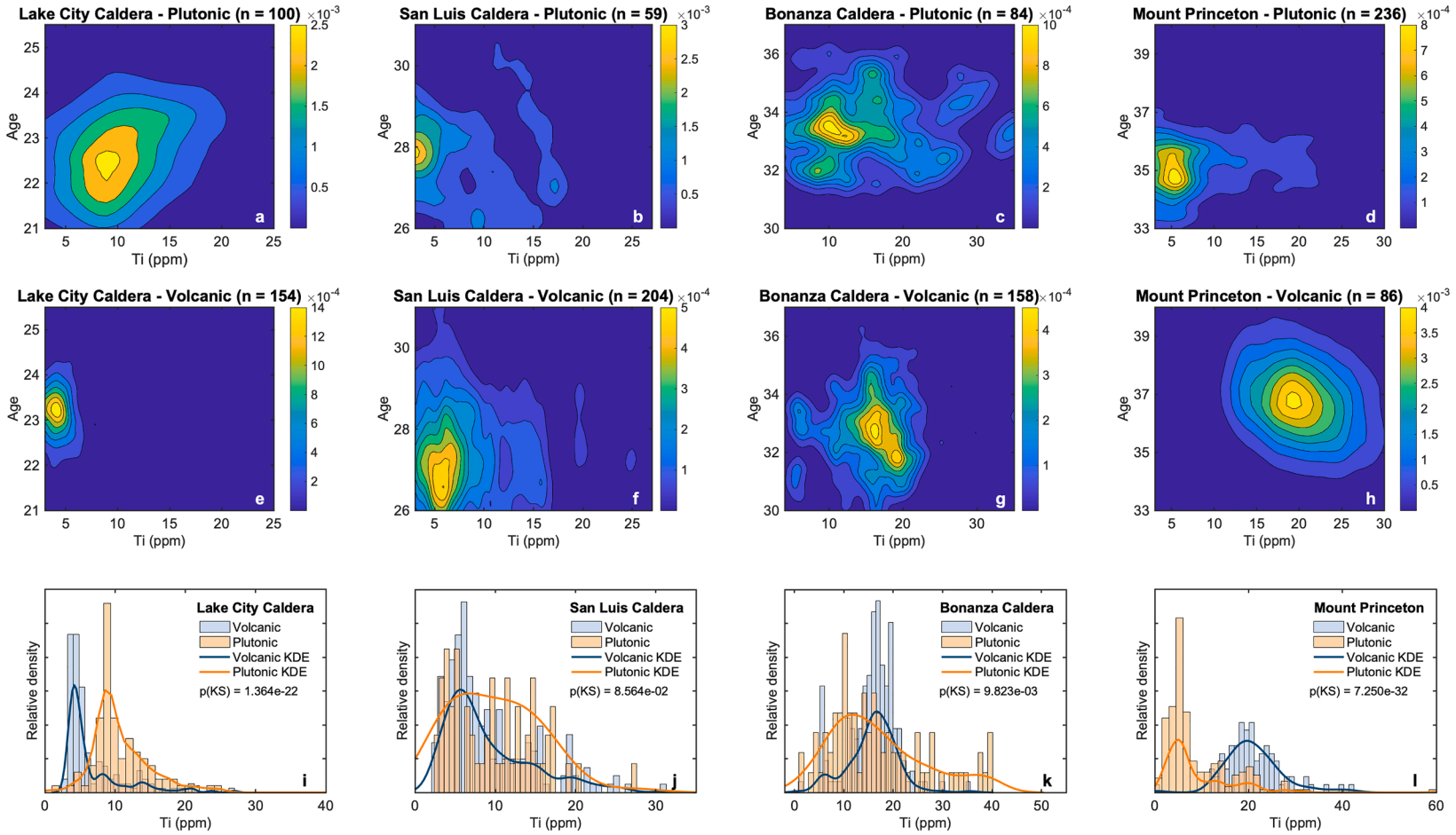

Fig. 2. Summary of LA-ICP-MS $^{206}Pb/^{238}U$ age and Ti content from zircons in plutonic and volcanic units from the Southern Rocky Mountain volcanic field (Lake City Caldera, San Luis Calera, Bonanza Caldera, Mt Princeton). (A-D) corresponds to combined age and Ti content density plots. (I-L) shows combined kernel density estimations (KDEs) and histograms. Result of Kolmogorov-Smirnov (KS) statistical analyses is shown as p (KS), with the low value indicating that the two populations are unlikely to be derived from the same underlying distribution.

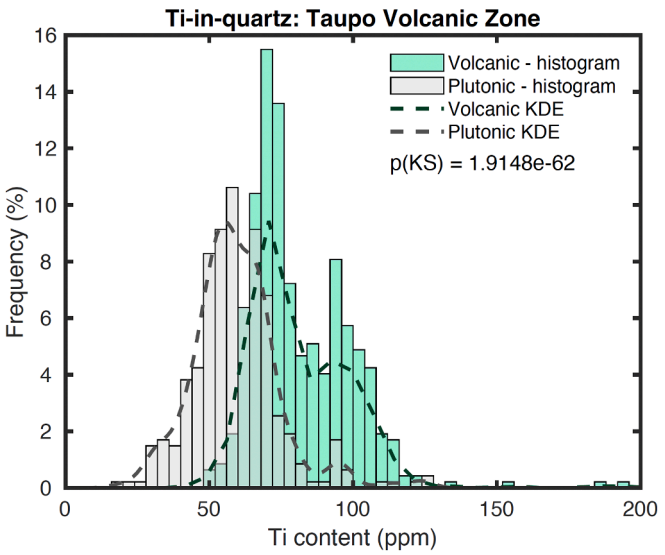

Fig. 3. Titanium distribution in quartz grains from volcanic (n = 471) and lithic plutonic (n = 343) samples from the Taupo Volcanic Zone shown as histograms and kernel density estimations (KDEs). Result of Kolmogorov-Smirnov (KS) statistical analyses is shown as p(KS), with the low value indicating that the two populations are unlikely to be derived from the same underlying distribution.

Our Ti distribution from crystallisation simulations shows that the size of the gap between volcanic and plutonic medians is controlled by a_{TiO2} and eruption temperature. Although crystallisation rate and eruption fraction affect the overall shape of the curves, they have no effect on the gap size (see Supplementary). At lower a_{TiO2} and/or lower eruption temperatures the gap becomes considerably smaller (Fig. 4), and it would likely be difficult to spot in natural examples, due to potential analytical limitations. This is likely the case at San Luis Caldera (Fig. 5), where a combined effect of lower aTiO2 and a small difference between eruption and solidus temperatures may have only produced a very small gap in the Ti distribution between the volcanic unit (Sunshine Peak Tuff) and its plutonic equivalent. For quartz, these conditions may be less crucial, as the absolute numbers are higher, facilitating the visual identification of a gap in Ti distribution: for instance, we simulated conditions that reproduce the TVZ distributions, and although they fit a scenario with low eruption temperature (Fig. 5), the gap is still very discernible. We note that while our models provide possible crystallisation conditions for some of the natural systems analysed in this study, illustrating the concept of non-equivalent Ti distributions in co-magmatic plutonic-volcanic units, they should not be seen as a perfect reproduction of nature.

4.2. Zircon Ti distribution in the rocks of the Pikes Peak region

The comparison between zircon Ti distributions in the Pikes Peak granite and the sub-volcanic Keeton Porphyry reveals a pattern similar to that observed in most of the modern volcanic-plutonic pairs: zircon crystals from the Keeton Porphyry show a pronounced shift towards higher Ti contents (Fig. 6).

Distributions of Ti concentrations in zircon from both the Pikes Peak granite and Tava sandstone are asymmetrical, with a high-density peak and a tail towards higher concentrations (Fig. 7). In the granite, Ti-in-zircon concentrations peak near 7 ppm and extend upwards to >30 ppm. In the Tava sandstone, the filtered zircon Ti distribution shows a peak at 11 ppm with a tail that extends to 40 ppm. Hence, the kernel density estimation (KDE) of the Tava Sandstone is shifted towards higher Ti contents than the Pikes Peak batholith (Fig. 7). The Kolmogorov-Smirnov (KS) test determines the probability of two populations being derived from the same underlying distribution (Press et al., 1988), when applied to both zircon populations this test yields a low value (p(KS) = 1.304e-8). This result ($p < 0.05$) allows to reject the null hypothesis that these populations are drawn from an identical underlying distribution, thus demonstrating that they are statistically distinct Ti groups.

4.3. Quartz Ti distribution in the rocks of the Pikes Peak region

4.3.1. Correlating CL intensity with Ti contents in the Tava sandstone

Blue band CL images of the Tava Sandstone (Fig. 1) show quartz crystals ranging from dark grey to completely white. Typically, dark crystals are larger and more abundant compared to bright crystals. Amongst the crystals measured via fs-LA-ICP-MS, darker crystals show Ti < 50 ppm, whereas bright crystals are generally above 150 ppm.

A number of studies have proposed a linear calibration between Ti content in quartz and CL intensity (Landtwing and Pettke, 2005; MacRae et al., 2010; Matthews et al., 2012; Leeman et al., 2012; Tavazzani et al., 2020). Following a similar approach, we derived a linear equation of Ti-in-quartz against blue-band CL grayscale (brightness) value from our dataset (Fig. 8):

$$\mathrm{Ti-in-quartz\ (ppm)} = 0.721 * \mathrm{GrayScale} - 6.828 \quad (1)$$

Where GrayScale stands for the grey value (from 0 to 255) retrieved from image analysis. Fig. 9 shows the Ti-in-quartz distribution in the analysed Tava thin section based on this calibration. The distribution of quartz grayscale values is highly non-linear, with a large proportion of both dark crystals (< 100 in grayscale) and of very bright crystals (255 in grayscale). The high percentage of bright crystals results from CL brightness and contrast limitations owing to this non-linear distribution: all crystals having Ti content greater than 177 ppm correspond to a GrayScale value of 255 and have completely white CL response. We note that CL grayscale always depends on the brightness and contrast settings during image acquisition, hence, when applying this technique to future studies, it will be necessary to adjust the calibration through a calibration dataset linking CL brightness to Ti contents directly measured by LA-ICP-MS.

The results of the calibration test (see Section 3.1 for details) show a similar distribution of Ti contents between values actually measured by fs-LA-ICP-MS and those determined using the CL-based calibration (Fig. 10). In terms of relative error, a larger error (30 %) is observed when comparing proportions of high-Ti quartz in the CL-based data from the Tava sandstone with the single grain-pattern validation data. Although significant, in absolute terms the deviation is small (1.2 %) and might be related to minor selection bias when placing analysis points, as bright crystals are often much smaller than dark ones and thus more likely to be missed, or to natural variations in the distribution of low, medium, and high-Ti grains across different areas of the sample.

4.3.2. Comparison between Pikes Peak granite and Tava sandstone

In the Tava sandstone, high-Ti grains (>177 ppm) account for ~ 3.5 % of the total quartz area in the thin section (Fig. 10). Grains <45 ppm Ti are grouped as low-Ti and make up to the majority (~72 %) of the analysed area. Visually, these low-Ti areas generally correspond to the larger grains in the analysed sample. These crystals are broadly considered as pegmatitic/hydrothermal, without any inference of the particular process of formation, because low Ti contents in the Pikes Peak granite are found only in (1) pegmatitic quartz or (2) in hydrothermal rims and fluid inclusions trails in quartz in the main granite (Fonseca Teixeira et al., 2022). Crystals ranging from 45 to 177 ppm Ti are considered medium-Ti and make up ~24 % of the thin section. We highlight that percentages are determined based on total quartz area in the thin section, as other phases were previously excluded.

When considering only grains designated magmatic in origin and excluding the contribution from purported hydrothermal crystals, medium-Ti quartz represents 87 % and high-Ti quartz represents 13 % of

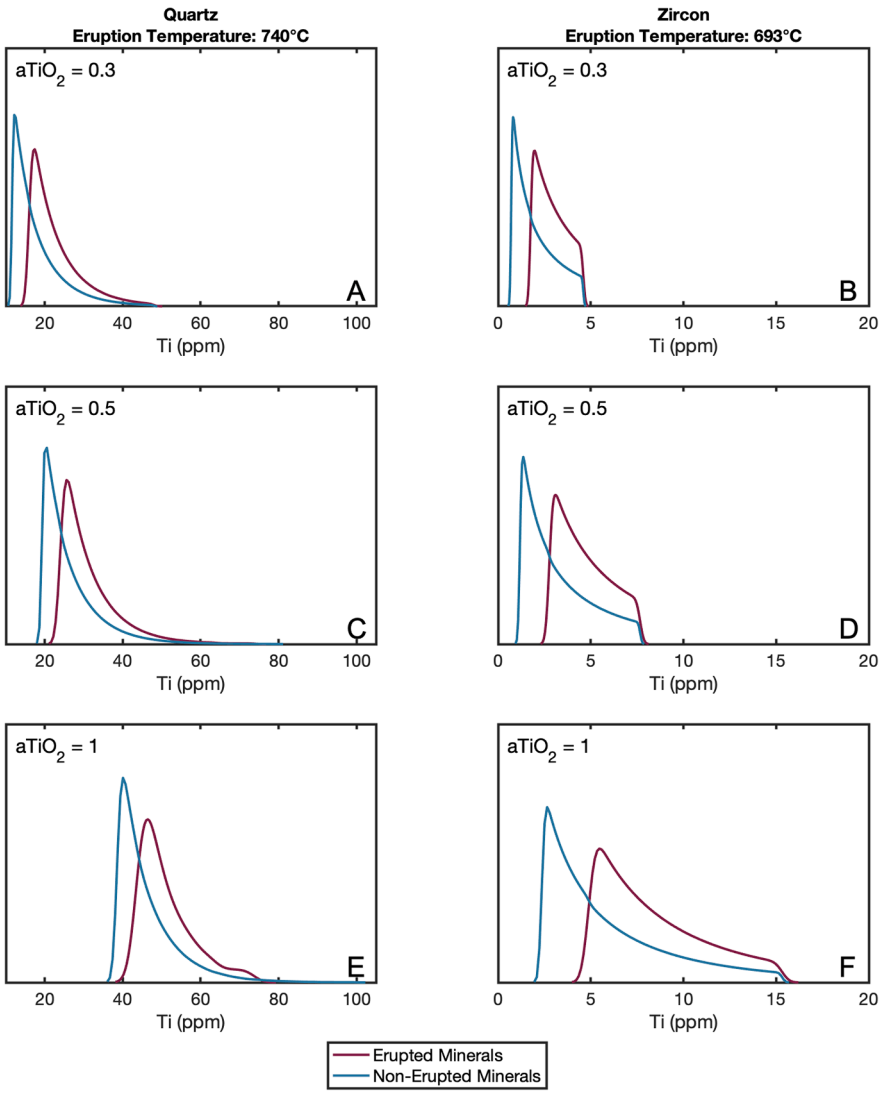

Fig. 4. Zircon and quartz crystallisation models for various $a\mathrm{TiO_2}$ at exponential crystallisation rate. Y axis displays the relative probability of a crystal with a certain Ti content (X axis) to be volcanic or plutonic, i.e. at lower Ti contents, crystals are more likely to be plutonic; at higher Ti contents they are more likely to be volcanic. Models are based on fixed values for pressure (4 kbar), silica activity ($a\mathrm{SiO_2} = 1$, for zircon), eruption fraction (5%), and eruption at 50% of crystallised zircons. Eruption is triggered at 750 C.

the sample (Fig. 4). In comparison, the Pikes Peak batholith quartz data (from Fonseca Teixeira, 2022) yields significantly less (~3 %) high-Ti quartz.

5. Discussion

5.1. The distinction between volcanic and plutonic crystals in silicic magmatic systems

To understand the systematic differences between volcanic and plutonic crystals sourced from a common system, we analysed the Ti distribution of zircons from four examples from SRMVF and TVZ. Our results show a clear statistical difference between the Ti distributions observed in some volcanic and plutonic samples (Mount Princeton, TVZ), in agreement with the original hypothesis that **volcanic crystals are expected to be richer in Ti in comparison to their plutonic relatives**. This difference is still present, although less obvious, in the Bonanza and San Luis calderas, but absent at the Lake City volcanic centre. The method proposed in this study implicitly assumes a simple cooling history and constant $a\mathrm{TiO_2}$ throughout the system's evolution, spanning from hot lavas to cooler hydrothermal pegmatites. This approach is over-simplistic, if anything because $a\mathrm{TiO_2}$ is known to change during the lifetime of a magmatic reservoir even in closed-system conditions (Fonseca Teixeira et al., 2023). Therefore, the possibility exists that under a specific set of circumstances Ti distributions in quartz and zircon may not follow our modelled distributions in volcanic and plutonic counterparts.

This is shown by the example of the Lake City magmatic system (Fig. 2a, e). In this case, the Ti distribution in plutonic zircon is statistically higher than in volcanic zircons. We propose two explanations for this counter-intuitive observation:

1) The Sunshine Peak Tuff (the volcanic unit from which zircons were analysed in the Lake City system), is an typical zoned ignimbrite, dominated in volume by extremely evolved, high-$\mathrm{SiO_2}$ rhyolite melt stored at low temperature. Therefore, crystallisation from this melt would generate low-Ti zircons (and quartz). The late-erupted part of the Sunshine Peak Tuff is however less evolved, more crystal-rich, and shows zircons with higher Ti contents overlapping with the plutonic unit, a quartz syenite intrusion interpreted as the left-over plutonic equivalent of the late-erupted Sunshine Peak Tuff (Lubbers et al., 2020).

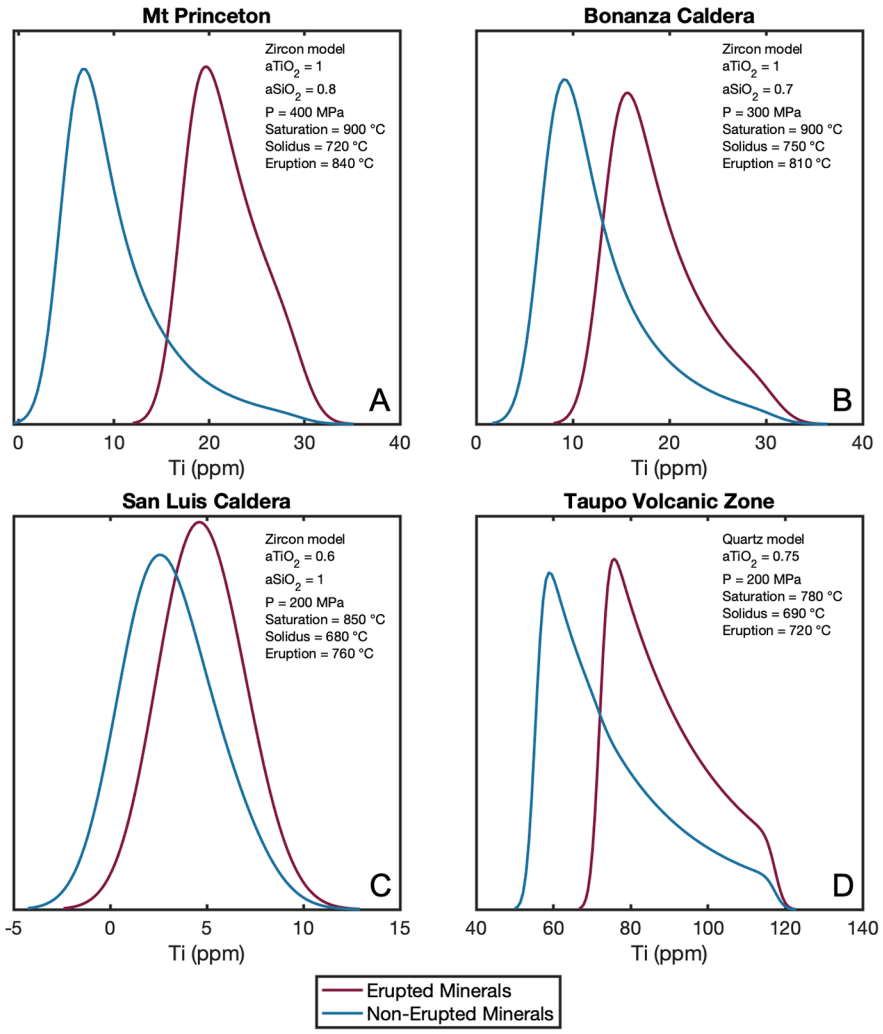

Fig. 5. Models simulating potential conditions on which the rocks from SRMVF and TVZ may have formed to match the curves observed in Figs. 2 and 3. See text and Supplementary material for further information on the model. The models here provided are one possible solution, and do not necessarily represent the only possibility to generate such curves.

2) Mafic recharge of Ti-rich magma after eruption of the Sunshine Peak Tuff, leading to resurgence of the quartz syenite pluton, was likely enriched in Ti, causing an increase the a_{TiO2}, as recorded by thin bright CL rims in plutonic quartz (Lubbers et al., 2020).

Application of this technique to sediments derived from a setting such as Lake City Caldera would lead to inconclusive results. This is because the absence of high-Ti crystals in the sediments does not rule out an eruption, only that the eruption is not recorded by Ti contents. Hence, this technique may successfully be used to determine if a pluton has erupted in the past, but it cannot determine if it has not (particularly if erupted material is a low-temperature high-SiO_2 rhyolite). While we anticipate these instances to be relatively infrequent (high SiO_2 rhyolites are a small fraction of volcanic units in most magmatic provinces; see for example Iceland(Gunnarsson et al., 1998), and the Cascade arc (Hildreth, 2007), we emphasize the importance of meticulously examining numerous crystals within plutonic rocks to determine the applicability of the proposed method and account for any complexities arising from disequilibrium growth (e.g. Matthews et al., 2012; Barbee et al., 2020). In fact, the technique has potential even without good constraints on either the magmatic history of the system or $a\mathrm{TiO_2}$, since the direct comparison of statistical distributions of Ti contents in plutonic vs. sedimentary quartz and zircon already informs on a similarity or difference in the proportions of high vs. low temperature crystals.

In general, we emphasize that our models and the data from SRMVF and TVZ demonstrate that (i) the difference between volcanic and plutonic crystals is related to their Ti-in-zircon/quartz statistical distribution, and not to their absolute Ti content; and (ii) a successful use of the approach applied to sedimentary zircon/quartz requires a good knowledge of the Ti distribution in plutonic zircon/quartz from which the sediment derived.

5.2. *Fingerprinting quartz and zircon provenance in the Tava sandstone*

As the Pikes Peak batholith is a rutile-saturated system (at least approaching the solidus, as demonstrated by Fonseca Teixeira et al., 2022) and Ti contents in quartz and zircon of the Pikes Peak batholith and the Keeton Porphyry are relatively high (Fig. 6; see also Fonseca Teixeira et al., 2022), $a\mathrm{TiO_2}$ is constrained to ~1. Thus, low, medium, and high-Ti populations can be broadly considered low (<695 °C), medium (695–865 °C), and high temperature (>865 °C, temperatures calculated using the calibration of Huang and Audétat, 2012). Our analyses reveal a significant fraction of low-Ti quartz into the investigated sediments. In the Pikes Peak batholith, low-Ti quartz only occurs in pegmatites or as hydrothermal rims and recrystallised fluid inclusion paths in the granitic quartz (Fonseca Teixeira et al., 2022). However, in the Tava Sandstone, evidence of such rims or trails is rarely observed, probably due to the scale of observation (i.e. fluid inclusions trails in

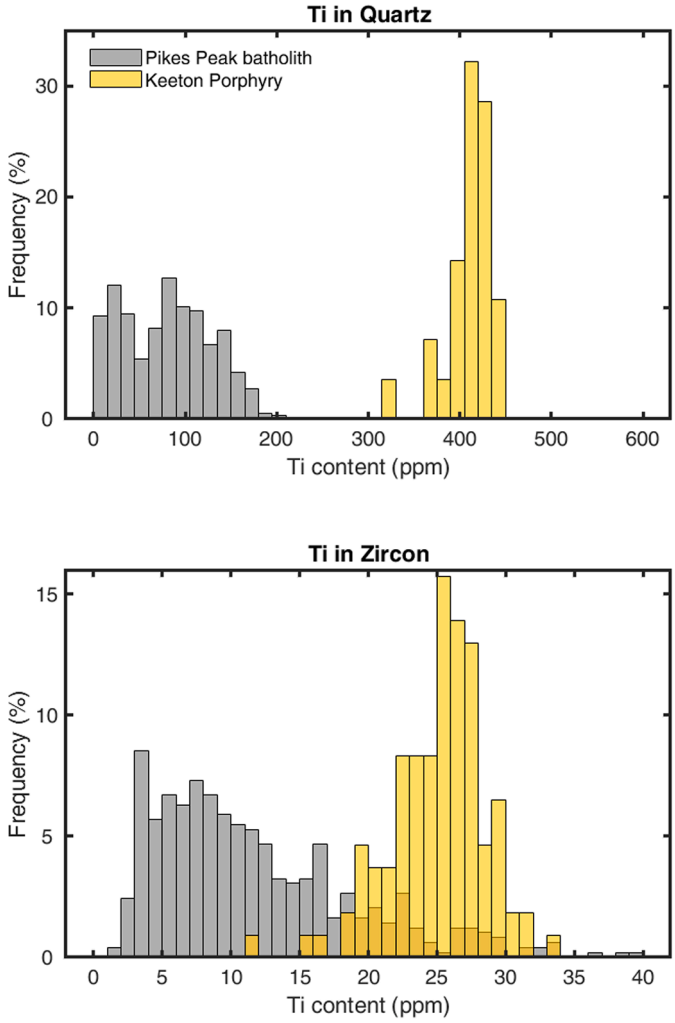

Fig. 6. Ti in quartz and Ti in zircon contents in the Keeton Porphyry and Pikes Peak batholith.

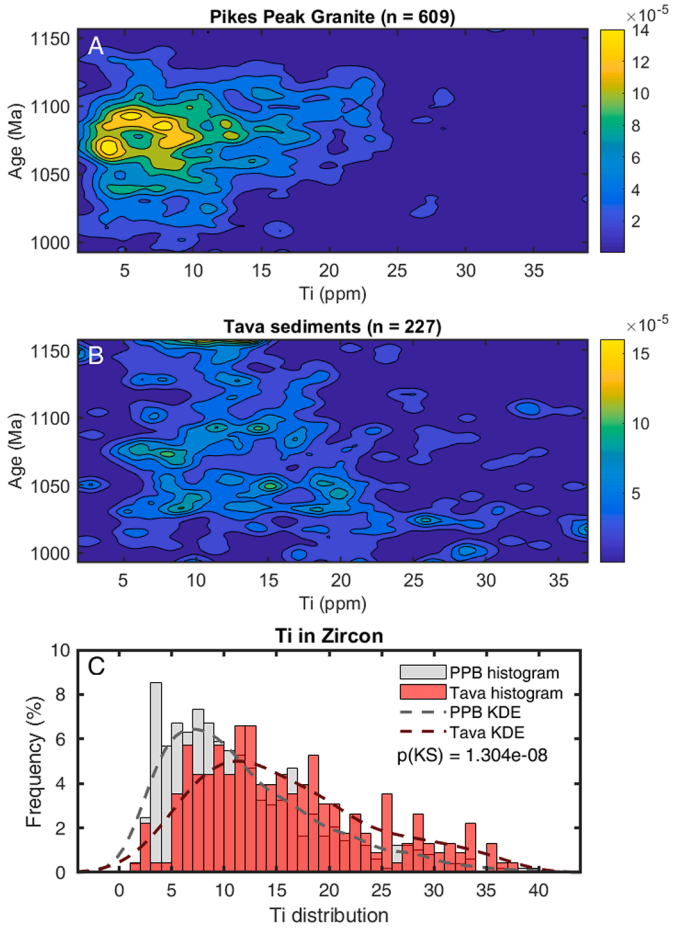

Fig. 7. (A) Pikes Peak granite zircon $^{206}Pb/^{238}U$ ages and Ti content (ppm). (B) Tava Sandstone detrital zircon $^{206}Pb/^{238}U$ ages and Ti content (ppm). (C) Ti-in-zircon distribution of the Pikes Peak granite (PPB, $n = 492$) and Tava Sandstone ($n = 227$) shown as histograms and kernel density estimations (KDEs). Result of Kolmogorov-Smirnov (KS) statistical analyses is shown as p(KS), with the low value indicating that the two populations are unlikely to be derived from the same underlying distribution.

individual crystals are likely too thin to be visible in a full thin section image) or due to breakage of crystals during erosion and sedimentary transport. Thus, we consider a majority of low-Ti quartz to be of pegmatitic origin.

In the case of zircon, pegmatitic zircon crystals are known for their enrichment in U and REE, are commonly metamict and fail to provide accurate age information (e.g. Hoskin, 2005; Yin et al., 2013). Our age filtering procedure automatically excluded zircons of this sort because they fell outside the Pikes Peak age bracket, likely due to lead loss. Therefore, the statistical distribution of Ti in zircon observed in the Tava Sandstone reflects minimal to no contribution of zircon from pegmatitic environments.

Several factors may have led to an elevated pegmatitic input into the Tava Sandstone:

(1) The siliciclastic source of Tava injectites likely was proximal to pegmatite exposures in the Pikes Peak region, so that a substantial component of pegmatitic minerals was introduced into the sedimentary system.
(2) Large pegmatitic quartz crystals may have withstood mechanical erosion and been incorporated in higher proportion in Tava source sediments.
(3) Quartz constitutes a volumetrically significant proportion of zoned pegmatites with massive quartz cores (consisting almost entirely of quartz), in contrast to 30 % in typical granite

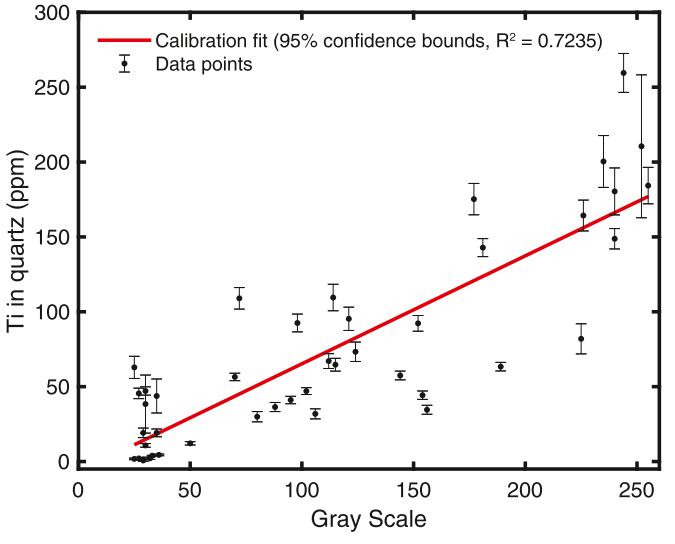

Fig. 8. Calibration fit based on LA-ICP-MS measurements of Ti in quartz and corresponding grey colour in the CL image. Black CL corresponds to "0"; white CL corresponds to "255".

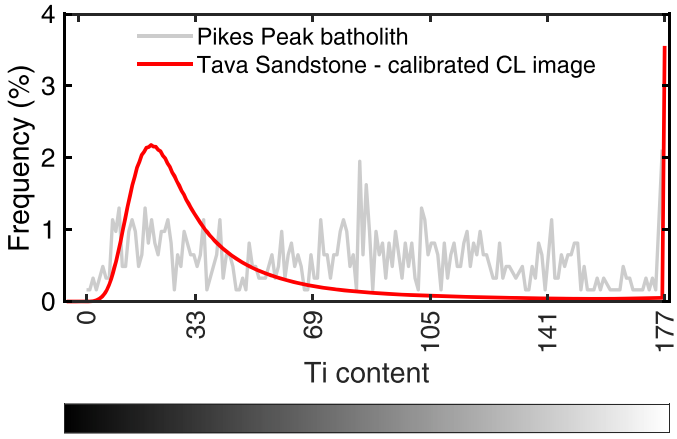

Fig. 9. Colour histogram of the total quartz area in a full thin section (same section as shown in Fig. 1), calibrated to show distribution of Ti contents in quartz (ppm) from the Tava sandstone (in red) and Ti content distribution in quartz from the Pikes Peak batholith (in grey; data from Fonseca Teixeira et al., 2022) for comparison.

compositions (Johannes and Holtz, 2012). In a theoretical scenario, an equivalent eroded volume of pegmatite would contribute twice as much quartz as granite. While such was not the case for the Pikes Peak batholith where granites are volumetrically dominant, it highlights how the contributed volume does not always directly relate to the source volume .

Once pegmatitic quartz grains(<45 ppm of Ti) are excluded, Tava Sandstone displays a greater abundance of high-temperature quartz (>177 ppm of Ti), reaching nearly four times the high-Ti quartz proportion in the Pikes Peak batholith. The implication is that the Tava Sandstone contains quartz crystallised in a hotter environment. The zircon Ti distribution in the Tava Sandstone exhibits a shift towards higher Ti contents compared to the Pikes Peak batholith (Fig. 7), indicating the possible contribution of a source of similar age as the batholith but containing zircons with higher Ti contents. We consider it likely that the higher temperature, higher-Ti igneous source was a comagmatic erupted phase.

5.3. *Contribution of high-Ti crystals to the Tava sandstone: volcanic activity in the Pikes Peak system*

Quartz and zircon Ti distributions exhibit a higher proportion of high-Ti crystals in Tava Sandstone than in Pikes Peak batholith. U-Pb dates on euhedral zircon fall within our 1000–1150 Ma age filter, making it plausible that the zircon originated from a volcanic unit of the batholith's magmatic system, that is absent from or under-represented at the current level of exposure. These units were eroded prior to the ~676 Ma formation (Jensen et al., 2018) of the Tava injectites. We therefore consider the proximal Tava sandstone to preserve an indirect record of lavas or ignimbrites of Pikes Peak age that are absent from the region today.

One subvolcanic, comagmatic remnant of Pikes Peak age is the Keeton Porphyry (Sanders, 1999), which provides evidence that the Pikes Peak system was not exclusively plutonic. The Keeton Porphyry displays consistently high Ti contents in quartz (400–430 ppm) and zircon (20–25 ppm - Fig. 6). Based on this evidence, we conclude that the Pikes Peak's magmatic system likely underwent one or several eruptive event(s), generating silicic volcanic materials with geochemical affinity to the Keeton porphyry (bearing high-Ti quartz and zircon), whose subsequent preferential erosion contributed to the formation of the Tava Sandstone.

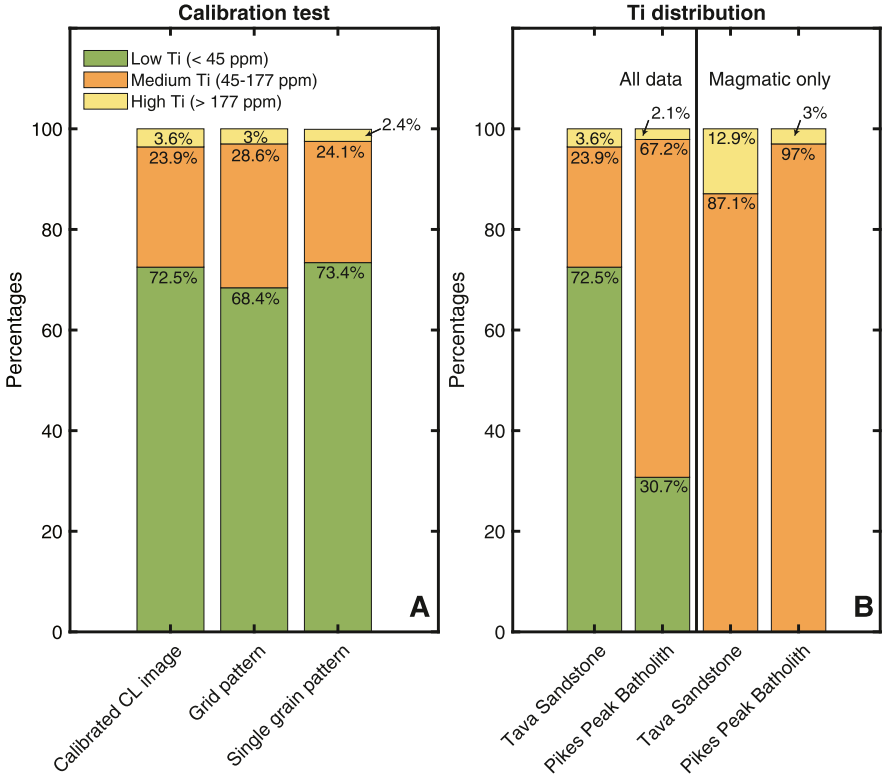

Fig. 10. A) Ti distribution in quartz in the Tava Sandstone, obtained by this study's CL-calibration and in validation LA-ICP-MS data. B) Comparison between proportions of low, medium, and high-Ti quartz in the Pikes Peak batholith and Tava Sandstone.

6. Outlook: how to locate volcanic centres that have been completely eroded?

Our study sheds light on the significance of sedimentary-hosted quartz and zircon as potential recorders of eruptive activity throughout Earth's magmatic history. With the rationale that volcanic and plutonic quartz/zircon should show different Ti distributions owing to the distinct thermal histories of erupted vs. unerupted magmatic units, we develop a new approach based on a comparison of Ti distributions between exposed plutonic and sedimentary quartz/zircon to assess the likelihood of a now-eroded volcanic counterpart to ancient plutonic systems. Although the tests on recent, well-constrained volcanic-plutonic systems (SRMVF and TVZ) show that the working hypothesis is generally valid, the specific chemical affinity (i.e. $a\mathrm{TiO_2}$) and magmatic evolution of each system complexifies the picture (see below).

We apply this method to the Tava Sandstone, a proximal sedimentary unit that records a detrital contribution from high-Ti quartz and zircon, which are not observed in the Pikes Peak granite itself and possibly derived from volcanic units. This finding suggests that our method holds promise as a means to discriminate "missing" magmatic sources by means of quartz and zircon in sedimentary units. Expanding our approach to sedimentary provenance studies will open new avenues for refining the magmatic history of continental crust through sedimentary formations.

The benchmark for new applications is the source pluton, characterised in terms of zircon and quartz Ti content distributions. On this basis, one can assess how different the detrital zircon and quartz Ti distributions are and, in turn, likelihood of input of volcanic material. Considering the examples from SRMVF, and the discussed potential problems regarding aTiO2, we caution against use of our technique on systems marked by:

(1) very low Ti in quartz and zircon (due to low $a\mathrm{TiO_2}$ or low crystallisation temperatures), as the volcanic-plutonic gap may become too small to be identified with currently available analytical technology.
(2) recharge from a Ti-rich melt, as it can increase $a\mathrm{TiO_2}$. Evidence of recharge may be indicated by bright CL rims upon quartz crystals in the plutonic rocks.

The techniques introduced here will be more readily applied to systems with higher quartz and zircon saturation temperatures (e.g. A-type systems) or higher $a\mathrm{TiO_2}$. Application to systems with cooler crystallisation temperatures (e.g. wet arc magmas) may be explored, provided that the source granite is the baseline to be carefully analysed for its suitability. In examples where Ti concentrations are very low, we suggest the use of additional elements that record fractionation (e.g. Hf, Th/U; see Yan et al., 2018).

Although our study compares currently exposed plutonic and volcanic units, in reality, the volcanics that exist may not represent the full range of erupted materials, which may include lavas and ignimbrites with a wide range of compositions. The more silicic extrusive units might be more similar to the exposed plutonic lithologies, but less differentiated lavas if present could also appear in the detrital record, with distinct and variable Ti content. Finally, we stress that while our technique can be used to identify plutons that had associated volcanic rocks, it cannot be used to unambiguously determine plutons that did not erupt.

In summary, our CL-based calibration successfully reproduces proportions of pegmatitic and plutonic contribution in the sedimentary rocks. Hence, the present technique can be used to understand sedimentary provenance and to quantify contributions from known magmatic sources with well quantified Ti-contents. If multiple systems contribute to sediments, the technique can still be used but only to distinguish rocks with quartz of different Ti contents, rather than temperature, due to potential differences in $a\mathrm{TiO_2}$. This can be done by selecting potential contributors (i.e. any quartz bearing rock in the region) and analysing their quartz crystals, which then can be matched with the results quantified from the image coupled with the CL calibration.

Understanding of the connections between silicic volcanic and plutonic realms requires analyses of examples that bridge these domains. The novel approach of exploring sediments as potential reservoirs of information about eroded volcanic units offers a promising avenue for our comprehension of the volcanic-plutonic connection. This new perspective holds the potential to further characterise the chemical evolution and growth of the Earth's crust throughout time.

CRediT authorship contribution statement

L.M. Fonseca Teixeira: Writing – original draft, Visualization, Methodology, Investigation, Formal analysis, Conceptualization. **O. Laurent:** Writing – review & editing, Methodology, Investigation, Conceptualization. **J. Troch:** Writing – review & editing, Supervision. **C. S. Siddoway:** Writing – review & editing, Resources. **L. Tavazzani:** Writing – review & editing, Investigation. **C. Deering:** Writing – review & editing, Resources, Investigation. **O. Bachmann:** Writing – review & editing, Supervision, Conceptualization.

Declaration of competing interest

The authors declare that they have no known competing financial interests or personal relationships that could have appeared to influence the work reported in this paper.

Data availability

Data is available on the Supplementary Material.

Acknowledgments

This research was supported by the Grubermann-Burri funds of the ETH (covered LMFT). We thank Françoise Maubé and Julien Berger for assistance and discussion relative to the acquisition of SEM images; and Aurélie Marquet and Mathieu Leisen for help with fs-LA-ICP-MS analyses at GET-OMP Toulouse; as well as Roman Klinghardt for the assistance with the EPMA at RWTH Aachen University. We are grateful to YingQi Wong for providing some assistance with MATLAB and calculations, and to Jakub Sliwinski for sharing his samples from Colorado SRMVF with us and for helpful discussions. We thank Calvin Miller and Madison Myers for the reviews that helped improving the quality of this work, and Chiara M. Petrone for editorial handling.

Supplementary materials

Supplementary material associated with this article can be found, in the online version, at doi:10.1016/j.epsl.2024.118906.

References

Bachmann, O., Huber, C., 2016. Silicic magma reservoirs in the Earth's crust. Am. Mineral. 101, 2377–2404. https://doi.org/10.2138/am-2016-5675 v.
Bachmann, O., Miller, C.F., de Silva, S.L., 2007. The volcanic–plutonic connection as a stage for understanding crustal magmatism. J. Volcanol. Geotherm. Res. 167, 1–23. https://doi.org/10.1016/j.jvolgeores.2007.08.002 v.
Barbee, O., Chesner, C., Deering, C., 2020. Quartz crystals in Toba rhyolites show textures symptomatic of rapid crystallization. Am. Mineral. 105, 194–226. https://doi.org/10.2138/am-2020-6947 v.
Barker, F., Wones, D.R., Sharp, W.N., Desborough, G.A., 1975. The Pikes Peak batholith, Colorado front range, and a model for the origin of the gabbro—Anorthosite—Syenite—Potassic granite suite. Precambrian Res. 2, 97–160. https://doi.org/10.1016/0301-9268(75)90001-7 v.
Barth, S., Oberli, F., Meier, M., Blattner, P., Bargossi, G.M., Di Battistini, G., 1993. The evolution of a calc-alkaline basic to silicic magma system: geochemical and Rb-Sr,

Sm-Nd, and 18O16O isotopic evidence from the Late Hercynian Atesina-Cima d'Asta volcano-plutonic complex, northern Italy. Geochim. Cosmochim. Acta 57, 4285–4300. https://doi.org/10.1016/0016-7037(93)90323-O v.
Brown, S.J.A., Burt, R.M., Cole, J.W., Krippner, S.J.P., Price, R.C., Cartwright, I., 1998. Plutonic lithics in ignimbrites of Taupo Volcanic Zone, New Zealand; sources and conditions of crystallisation. Chem. Geol. 148, 21–41. https://doi.org/10.1016/S0009-2541(98)00026-6 v.
Clemens, J.D., Bryan, S.E., Mayne, M.J., Stevens, G., Petford, N., 2022. How are silicic volcanic and plutonic systems related? Part 1: a review of geological and geophysical observations, and insights from igneous rock chemistry. Earth. Sci. Rev. 235, 104249 https://doi.org/10.1016/j.earscirev.2022.104249 v.
Crisp, J.A., 1984. Rates of magma emplacement and volcanic output. J. Volcanol. Geotherm. Res. 20, 177–211. https://doi.org/10.1016/0377-0273(84)90039-8 v.
Crisp, L.J., Berry, A.J., Burnham, A.D., Miller, L.A., Newville, M., 2023. The Ti-in-zircon thermometer revised: the effect of pressure on the Ti site in zircon. Geochim. Cosmochim. Acta. https://doi.org/10.1016/j.gca.2023.04.031.
De Silva, S., Zandt, G., Trumbull, R., Viramonte, J., 2006. Large-scale silicic volcanism - the result of thermal maturation of the crust. In: Advances in Geosciences, 1. World Scientific Publishing Company, Advances in Geosciences, pp. 215–230. https://doi.org/10.1142/9789812707178_0021. Volume 1, v. Volume.
Deering, C.D., Keller, B., Schoene, B., Bachmann, O., Beane, R., Ovtcharova, M., 2016. Zircon record of the plutonic-volcanic connection and protracted rhyolite melt evolution. Geology 44, 267–270. https://doi.org/10.1130/G37539.1 v.
Delph, J.R., Ward, K.M., Zandt, G., Ducea, M.N., Beck, S.L., 2017. Imaging a magma plumbing system from MASH zone to magma reservoir. Earth Planet. Sci. Lett. 457, 313–324. https://doi.org/10.1016/j.epsl.2016.10.008 v.
Ellis, B.S., Bachmann, O., Wolff, J.A., 2014. Cumulate fragments in silicic ignimbrites: the case of the Snake River Plain. Geology 42, 431–434. https://doi.org/10.1130/G35399.1 v.
Farina, F., Weber, G., Hartung, E., Rubatto, D., Forni, F., Luisier, C., Caricchi, L., 2024. Magma flux variations triggering shallow-level emplacement of the Takidani pluton (Japan): insights into the volcanic-plutonic connection. Earth Planet. Sci. Lett. 635, 118688 https://doi.org/10.1016/j.epsl.2024.118688 v.
Ferry, J.M., Watson, E.B., 2007. New thermodynamic models and revised calibrations for the Ti-in-zircon and Zr-in-rutile thermometers. Contrib. Mineral. Petrol. 154, 429–437. https://doi.org/10.1007/s00410-007-0201-0 v.
Fonseca Teixeira, L.M., Troch, J., Allaz, J., Bachmann, O., 2022. Magmatic to hydrothermal conditions in the transition from the A-type Pikes Peak granite (Colorado) to its related pegmatite. Front. Earth. Sci. (Lausanne) 10 v. https://www.frontiersin.org/articles/10.3389/feart.2022.976588. accessed July 2023.
Fonseca Teixeira, L.M., Troch, J., Bachmann, O., 2023. The dynamic nature of aTiO2: implications for Ti-based thermometers in magmatic systems. Geology. https://doi.org/10.1130/G51587.1.
Glazner, A.F., Coleman, D.S., Mills, R.D., 2018. The volcanic-plutonic connection. In: Breitkreuz, C., Rocchi, S. (Eds.), Physical Geology of Shallow Magmatic Systems: Dykes, Sills and Laccoliths. Springer International Publishing, Advances in Volcanology, Cham, pp. 61–82. https://doi.org/10.1007/11157_2015_11.
Graeter, K.A., Beane, R.J., Deering, C.D., Gravley, D., Bachmann, O., 2015. Formation of rhyolite at the Okataina Volcanic Complex, New Zealand: new insights from analysis of quartz clusters in plutonic lithics. Am. Mineral. 100, 1778–1789. https://doi.org/10.2138/am-2015-5135 v.
Gunnarsson, B., Marsh, B.D., Taylor, H.P., 1998. Generation of Icelandic rhyolites: silicic lavas from the Torfajökull central volcano. J. Volcanol. Geotherm. Res. 83, 1–45. https://doi.org/10.1016/S0377-0273(98)00017-1 v.
Hartung, E., Caricchi, L., Floess, D., Wallis, S., Harayama, S., 2021. Establishing genetic relationships between the Takidani Pluton and two large silicic eruptions in the Northern Japan Alps. J. Petrol. 62, egab085. https://doi.org/10.1093/petrology/egab085 v.
Heiken, G., Goff, F., Gardner, J.N., Baldridge, W.S., Hulen, J.B., Nielson, D.L., Vaniman, D., 1990. The Valles/Toledo Caldera complex, Jemez volcanic field, New Mexico. Annu. Rev. Earth Planet Sci. 18, 27–53. https://doi.org/10.1146/annurev.ea.18.050190.000331 v.
Heise, W., Caldwell, T.G., Bibby, H.M., Bennie, S.L., 2010. Three-dimensional electrical resistivity image of magma beneath an active continental rift, Taupo Volcanic Zone, New Zealand. Geophys. Res. Lett. 37 https://doi.org/10.1029/2010GL043110 v.
Hildreth, W., 2007. Quaternary magmatism in the Cascades. Geol. Perspect.
Hoskin, P.W.O., 2005. Trace-element composition of hydrothermal zircon and the alteration of Hadean zircon from the Jack Hills, Australia. Geochim. Cosmochim. Acta 69, 637–648. https://doi.org/10.1016/j.gca.2004.07.006 v.
Huang, R., Audétat, A., 2012. The titanium-in-quartz (TitaniQ) thermobarometer: a critical examination and re-calibration. Geochim. Cosmochim. Acta 84, 75–89. https://doi.org/10.1016/j.gca.2012.01.009 v.
Jensen, J.L., Siddoway, C.S., Reiners, P.W., Ault, A.K., Thomson, S.N., Steele-MacInnis, M., 2018. Single-crystal hematite (U–Th)/He dates and fluid inclusions document widespread Cryogenian sand injection in crystalline basement. Earth Planet. Sci. Lett. 500, 145–155. https://doi.org/10.1016/j.epsl.2018.08.021 v.
Johannes, W., Holtz, F., 2012. Petrogenesis and Experimental Petrology of Granitic Rocks, 22. Springer Science & Business Media v.
Jonk, R., 2010. Sand-rich injectites in the context of short-lived and long-lived fluid flow. Basin Res. 22, 603–621. https://doi.org/10.1111/j.1365-2117.2010.00471.x v.
Karakas, O., Wotzlaw, J.-F., Guillong, M., Ulmer, P., Brack, P., Economos, R., Bergantz, G.W., Sinigoi, S., Bachmann, O., 2019. The pace of crustal-scale magma accretion and differentiation beneath silicic caldera volcanoes. Geology 47, 719–723. https://doi.org/10.1130/G46020.1 v.
Kennedy, B., Stix, J., 2007. Magmatic Processes Associated With Caldera Collapse At Ossipee Ring Dyke, 119. GSA Bulletin, New Hampshire, pp. 3–17. https://doi.org/10.1130/B25980.1 v.
Landtwing, M.R., Pettke, T., 2005. Relationships between SEM-cathodoluminescence response and trace-element composition of hydrothermal vein quartz. Am. Mineral. 90, 122–131. https://doi.org/10.2138/am.2005.1548 v.
Laurent, O., Björnsen, J., Wotzlaw, J.-F., Bretscher, S., Pimenta Silva, M., Moyen, J.-F., Ulmer, P., Bachmann, O., 2020. Earth's earliest granitoids are crystal-rich magma reservoirs tapped by silicic eruptions. Nat. Geosci. 13, 163–169. https://doi.org/10.1038/s41561-019-0520-6 v.
Laurent, O., Moyen, J.-F., Wotzlaw, J.-F., Björnsen, J., Bachmann, O., 2022. Early Earth zircons formed in residual granitic melts produced by tonalite differentiation. Geology 50, 437–441. https://doi.org/10.1130/G49232.1 v.
Leeman, W.P., MacRae, C.M., Wilson, N.C., Torpy, A., Lee, C.-T.A., Student, J.J., Thomas, J.B., Vicenzi, E.P., 2012. A study of cathodoluminescence and trace element compositional zoning in natural quartz from volcanic rocks: mapping titanium content in quartz. Microsc. Microanal. 18, 1322–1341. https://doi.org/10.1017/S1431927612013426 v.
Lipman, P.W., 2007. Incremental assembly and prolonged consolidation of Cordilleran magma chambers: evidence from the Southern Rocky Mountain volcanic field. Geosphere 3, 42–70. https://doi.org/10.1130/GES00061.1 v.
Lipman, P.W., Sawyer, D.A., 1988. Preliminary geology of the San Luis Peak quadrangle and adjacent areas San Juan volcanic field, southwestern Colorado. US Geol. Surv.
Lipman, P.W., Zimmerer, M.J., McIntosh, W.C., 2015. An ignimbrite caldera from the bottom up: exhumed floor and fill of the resurgent Bonanza caldera, Southern Rocky Mountain volcanic field, Colorado. Geosphere 11, 1902–1947. https://doi.org/10.1130/GES01184.1 v.
Loucks, R.R., Fiorentini, M.L., Henríquez, G.J., 2020. New magmatic oxybarometer using trace elements in Zircon. J. Petrol. 61, egaa034. https://doi.org/10.1093/petrology/egaa034 v.
Lubbers, J., Deering, C., Bachmann, O., 2020. Genesis of rhyolitic melts in the upper crust: fractionation and remobilization of an intermediate cumulate at Lake City caldera, Colorado, USA. J. Volcanol. Geotherm. Res. 392, 106750 https://doi.org/10.1016/j.jvolgeores.2019.106750 v.
MacRae, C.M., Wilson, N.C., Leeman, W., Vicenzi, E., Torpy, A., Vasyukova, O., Goemann, K., Hasalova, P., 2010. An investigation into the general applicability of quantification of trace Ti in quartz by cathodoluminescence. Microsc. Microanal. 16, 808–809. https://doi.org/10.1017/S1431927610054772 v.
Martins Lino, L., Quiroz-Valle, F.R., Stipp Basei, M.Â., Farias Vlach, S.R., Hueck, M., Willbold, M., Brandolise Citroni, S., do Valle Lemos-Santos, D., 2023. Petrogenesis and tectonic significance of two bimodal volcanic stages from the Ediacaran Campo Alegre-Corupá Basin (Brazil): record of metacratonization during the consolidation of Western Gondwana. Precambrian Res. 385, 106950 https://doi.org/10.1016/j.precamres.2022.106950 v.
Matthews, N.E., Pyle, D.M., Smith, V.C., Wilson, C.J.N., Huber, C., van Hinsberg, V., 2012. Quartz zoning and the pre-eruptive evolution of the ~340-ka Whakamaru magma systems, New Zealand. Contrib. Mineral. Petrol. 163, 87–107. https://doi.org/10.1007/s00410-011-0660-1 v.
Metcalf, R.V., Smith, E.I., Walker, J.D., Reed, R.C., Gonzales, D.A., 1995. Isotopic disequilibrium among commingled hybrid magmas: evidence for a two-stage magma mixing-commingling process in the Mt. Perkins Pluton, Arizona. J. Geol. 103, 509–527. https://doi.org/10.1086/629773 v.
Miller, J.S., Matzel, J.E.P., Miller, C.F., Burgess, S.D., Miller, R.B., 2007. Zircon growth and recycling during the assembly of large, composite arc plutons. J. Volcanol. Geotherm. Res. 167, 282–299. https://doi.org/10.1016/j.jvolgeores.2007.04.019 v.
Müller, A., Wiedenback, M., Kerkhof, A.M.V.D., Kronz, A., Simon, K., 2003. Trace elements in quartz - a combined electron microprobe, secondary ion mass spectrometry, laser-ablation ICP-MS, and cathodoluminescence study. Eur. J. Mineral. 15, 747–763. https://doi.org/10.1127/0935-1221/2003/0015-0747 v.
Oliveros, V., Féraud, G., Aguirre, L., Fornari, M., Morata, D., 2006. The Early Andean Magmatic Province (EAMP): 40Ar/39Ar dating on Mesozoic volcanic and plutonic rocks from the Coastal Cordillera, northern Chile. J. Volcanol. Geotherm. Res. 157, 311–330. https://doi.org/10.1016/j.jvolgeores.2006.04.007 v.
Osborne, Z.R., Thomas, J.B., Nachlas, W.O., Angel, R.J., Hoff, C.M., Watson, E.B., 2022. TitaniQ revisited: expanded and improved Ti-in-quartz solubility model for thermobarometry. Contrib. Mineral. Petrol. 177, 31. https://doi.org/10.1007/s00410-022-01896-8 v.
Pamukçu, A.S., Schoene, B., Deering, C.D., Keller, C.B., Eddy, M.P., 2022. Volcano-pluton connections at the Lake City magmatic center (Colorado, USA). Geosphere 18, 1435–1452. https://doi.org/10.1130/GES02467.1 v.
Press, W.H., Vetterling, W.T., Teukolsky, S.A., Flannery, B.P., 1988. Numerical Recipes. Citeseer.
Quick, J.E., Sinigoi, S., Peressini, G., Demarchi, G., Wooden, J.L., Sbisà, A., 2009. Magmatic plumbing of a large Permian caldera exposed to a depth of 25 km. Geology 37, 603–606. https://doi.org/10.1130/G30003A.1 v.
Rozel, A.B., Golabek, G.J., Jain, C., Tackley, P.J., Gerya, T., 2017. Continental crust formation on early Earth controlled by intrusive magmatism. Nature 545, 332–335. https://doi.org/10.1038/nature22042 v.
Rusk, B.G., Reed, M.H., Dilles, J.H., Kent, A.J.R., 2006. Intensity of quartz cathodoluminescence and trace-element content in quartz from the porphyry copper deposit at Butte, Montana. Am. Mineral. 91, 1300–1312. https://doi.org/10.2138/am.2006.1984 v.
Sanders, A., 1999. Age of the Keeton Porphyry and Clast Lithologies Within the Pennsylvanian Fountain Formation: Implications for the Composition of the Upper Pikes Peak Batholith. Colorado College, Front Range, Colorado, p. 105.

Siddoway, C., 2023, Structural control upon the preservation of a Snowball Earth sedimentary record in Colorado, *in* v. 56 (4), 10.1130/abs/2024CD-399780.
Siddoway, C.S., Gehrels, G.E., 2014. Basement-hosted sandstone injectites of Colorado: a vestige of the Neoproterozoic revealed through detrital zircon provenance analysis. Lithosphere 6, 403–408. https://doi.org/10.1130/L390.1 v.
Siddoway, C., Myrow, P., and Fitz-Díaz, E., 2013, Strata, structures, and enduring enigmas: a 125th Anniversary appraisal of Colorado Springs geology, in Abbott, L.D. and Hancock, G.S. eds., Classic Concepts and New Directions: Exploring 125 Years of GSA Discoveries in the Rocky Mountain Region, Geological Society of America, v. 33, p. 0, 10.1130/2013.0033(13).
Siégel, C., Bryan, S.E., Allen, C.M., Gust, D.A., 2018. Use and abuse of zircon-based thermometers: a critical review and a recommended approach to identify antecrystic zircons. Earth. Sci. Rev. 176, 87–116. https://doi.org/10.1016/j.earscirev.2017.08.011 v.
Sliwinski, J.T., Guillong, M., Lipman, P.W., Zimmerer, M.J., Deering, C., Bachmann, O., 2022. Zircon U-Pb geochronology and trace element dataset from the Southern Rocky Mountain Volcanic Field, Colorado, USA. Data Brief 43, 108362. https://doi.org/10.1016/j.dib.2022.108362 v.
Smith, D.R., 1999. A review of the Pikes Peak batholith, Front Range, central Colorado: a "type example" of A-type granitic magmatism. Rocky Mountain Geol. 34, 289–312. https://doi.org/10.2113/34.2.289 v.
Spear, F.S., Wark, D.A., 2009. Cathodoluminescence imaging and titanium thermometry in metamorphic quartz. J. Metamorph. Geol. 27, 187–205. https://doi.org/10.1111/j.1525-1314.2009.00813.x v.
Stalder, R., Potrafke, A., Billström, K., Skogby, H., Meinhold, G., Gögele, C., Berberich, T., 2017. OH defects in quartz as monitor for igneous, metamorphic, and sedimentary processes. Am. Mineral. 102, 1832–1842. https://doi.org/10.2138/am-2017-6107 v.
Szymanowski, D., Ellis, B.S., Wotzlaw, J.-F., Bachmann, O., 2019. Maturation and rejuvenation of a silicic magma reservoir: high-resolution chronology of the Kneeling Nun Tuff. Earth Planet. Sci. Lett. 510, 103–115. https://doi.org/10.1016/j.epsl.2019.01.007 v.
Tavazzani, L., Peres, S., Sinigoi, S., Demarchi, G., Economos, R.C., Quick, J.E., 2020. Timescales and mechanisms of crystal-mush rejuvenation and melt extraction recorded in permian plutonic and volcanic rocks of the sesia magmatic system (Southern Alps, Italy). J. Petrol. 61, egaa049. https://doi.org/10.1093/petrology/egaa049 v.
Tavazzani, L., Wotzlaw, J.-F., Economos, R., Sinigoi, S., Demarchi, G., Szymanowski, D., Laurent, O., Bachmann, O., Chelle-Michou, C., 2023. High-precision zircon age spectra record the dynamics and evolution of large open-system silicic magma reservoirs. Earth Planet. Sci. Lett. 623, 118432 https://doi.org/10.1016/j.epsl.2023.118432 v.
Troch, J., Ellis, B.S., Schmitt, A.K., Bouvier, A.-S., Bachmann, O., 2018. The dark side of zircon: textural, age, oxygen isotopic and trace element evidence of fluid saturation in the subvolcanic reservoir of the Island Park-Mount Jackson Rhyolite, Yellowstone (USA). Contrib. Mineral. Petrol. 173, 54. https://doi.org/10.1007/s00410-018-1481-2 v.
Tweto, O., Kent, H., Porter, K., 1980. Precambrian Geology of Colorado: Colorado Geology. Rocky Mountain Association of Geologists, Denver, CO, pp. 37–46.
Wager, L.R., Brown, G.M., Wadsworth, W.J., 1960. Types of igneous cumulates. J. Petrol. 1, 73–85. https://doi.org/10.1093/petrology/1.1.73 v.
Wallrich, B.M., Miller, C.F., Gualda, G.A.R., Miller, J.S., Hinz, N.H., Faulds, J.E., 2023. Volcano-pluton connection: perspectives on material and process linkages, Searchlight pluton and Highland Range volcanic sequence, Nevada, USA. Earth. Sci. Rev. 238, 104361 https://doi.org/10.1016/j.earscirev.2023.104361 v.
Ward, K.M., Zandt, G., Beck, S.L., Christensen, D.H., McFarlin, H., 2014. Seismic imaging of the magmatic underpinnings beneath the Altiplano-Puna volcanic complex from the joint inversion of surface wave dispersion and receiver functions. Earth Planet. Sci. Lett. 404, 43–53. https://doi.org/10.1016/j.epsl.2014.07.022 v.
Wark, D.A., Watson, E.B., 2006. TitaniQ: a titanium-in-quartz geothermometer. Contrib. Mineral. Petrol. 152, 743–754. https://doi.org/10.1007/s00410-006-0132-1 v.
Wilson, C.J., Gravley, D., Leonard, G., Rowland, J., 2009. Volcanism in the Central Taupo Volcanic Zone, New Zealand: Tempo, Styles and Controls: Studies in Volcanology: the Legacy of George Walker, 2. Special Publications of IAVCEI, pp. 225–247 v.
Wilson, C.K., Jones, C.H., Gilbert, H.J., 2003. Single-chamber silicic magma system inferred from shear wave discontinuities of the crust and uppermost mantle, Coso geothermal area, California. J. Geophys. Res. 108 https://doi.org/10.1029/2002JB001798 v.
Wobus, R., Epis, R., Weimer, R., 1976. New data on potassic and sodic plutons of the Pikes Peak batholith, central Colorado. Stud. Colorado Field Geol. 8, 57–67 v.
Yan, L.-L., He, Z.-Y., Beier, C., Klemd, R., 2018. Zircon trace element constrains on the link between volcanism and plutonism in SE China. Lithos 320–321, 28–34. https://doi.org/10.1016/j.lithos.2018.08.040 v.
Yin, R., Wang, R.C., Zhang, A.-C., Hu, H., Zhu, J.C., Rao, C., Zhang, H., 2013. Extreme fractionation from zircon to hafnon in the Koktokay No. 1 granitic pegmatite, Altai, northwestern China. Am. Mineral. 98, 1714–1724. https://doi.org/10.2138/am.2013.4494 v.
Zimmerer, M.J., McIntosh, W.C., 2012. An investigation of caldera-forming magma chambers using the timing of ignimbrite eruptions and pluton emplacement at the Mt. Aetna caldera complex. J. Volcanol. Geotherm. Res. 245–246, 128–148. https://doi.org/10.1016/j.jvolgeores.2012.08.007 v.